Synchronized activity between the ventral hippocampus and the medial prefrontal cortex during anxiety

Avishek Adhikari[1], **Mihir A. Topiwala**[2], and **Joshua A. Gordon**[2,3]

[1]Department of Biological Sciences, Columbia University, New York, NY, 10032

[2]Department of Psychiatry, Columbia University, New York, NY, 10032

[3]The New York State Psychiatric Institute, New York, NY 10032

SUMMARY

The ventral hippocampus, unlike its dorsal counterpart, is required for anxiety-like behavior. The means by which it acts are unknown. We hypothesized that the hippocampus synchronizes with downstream targets that influence anxiety, such as the medial prefrontal cortex (mPFC). To test this hypothesis, we recorded mPFC and hippocampal activity in mice exposed to two anxiogenic arenas. Theta-frequency activity in the mPFC and ventral, but not dorsal hippocampus was highly correlated at baseline, and this correlation increased in both anxiogenic environments. Increases in mPFC theta power predicted avoidance of the aversive compartments of each arena, and were larger in serotonin 1A-receptor knockout mice, a genetic model of increased anxiety-like behavior. These results suggest a role for theta-frequency synchronization between the ventral hippocampus and the mPFC in anxiety. They are consistent with the notion that such synchronization is a general mechanism by which the hippocampus communicates with downstream structures of behavioral relevance.

INTRODUCTION

Anxiety in rodents is commonly modeled through paradigms such as the elevated plus maze (EPM) and the open field. Multiple lines of evidence, including lesion and local drug infusion studies, have shown that the hippocampus is necessary for normal anxiety-like behavior in these environments (Deacon et al., 2002; File et al., 1996). Recently, more selective lesions have demonstrated that the ventral (vHPC), but not the dorsal hippocampus (dHPC), is required for normal anxiety-related behavior (Bannerman et al., 2004; Kjelstrup et al., 2002). Although these reports implicate the vHPC, the mechanisms by which this structure exerts its role in anxiety are unknown. One possibility is that the vHPC influences the activity of downstream targets involved in anxiety modulation.

One such target region shown to be involved in anxiety is the medial prefrontal cortex (mPFC). The mPFC receives direct projections from the vHPC in both rats (Verwer et al., 1997) and mice (Parent et al., 2009), whereas its inputs from the dHPC are indirect, (Burwell R.D. and Witter, 2002; Hoover and Vertes, 2007). Numerous studies have demonstrated an important role for the mPFC in the modulation of anxiety, likely through its reciprocal connections with the amygdala and other limbic structures (Vertes, 2004). In addition to its well-characterized role in extinction of learned fear (Burgos-Robles et al., 2007), the mPFC may play a role in anxiety tests that require the hippocampus (Gonzalez et al., 2000; Lacroix et al., 2000; Shah et al., 2004; Shah and Treit, 2003) although there is some disagreement on this point in the literature (Corcoran and Quirk, 2007; Lacroix et al., 1998).

These findings suggest that the vHPC and mPFC might cooperate during anxiety. Previous reports have measured theta-frequency (4-12 Hz) synchronization between the hippocampus and downstream targets to demonstrate such cooperation during a variety of behaviors. Theta-frequency synchrony has been shown between the dHPC and the mPFC during working memory (Jones and Wilson, 2005), the striatum during learning (DeCoteau et al., 2007), and the amygdala during fear conditioning (Seidenbecher et al., 2003). Whether the vHPC might use a similar mechanism to synchronize with its targets is unclear. Consistent with this possibility, various lines of evidence have suggested that theta oscillations may play a role in anxiety. For example, anxiolytic agents decrease the propensity of the hippocampus to oscillate in the theta range (Zhu and McNaughton, 1994). Moreover, dorsal hippocampal theta power has been correlated with anxiety-related behavior in 5-HT1A receptor knockout mice (Gordon et al., 2005), a genetic model of enhanced anxiety (Heisler et al., 1998; Parks et al., 1998; Ramboz et al., 1998).

Taking into account these reports implicating theta oscillations, the vHPC and the mPFC, we hypothesized that synchronization in the theta range between the mPFC and the vHPC might underlie anxiety-like behavior. The present study tests this hypothesis by recording neural activity simultaneously from the mPFC, vHPC and dHPC in freely behaving mice during exploration of a familiar environment, a novel open field, and an elevated plus maze. In all environments, mPFC field potentials were more coherent with field potentials recorded from the vHPC than the dHPC. Exposure to either anxiogenic environment specifically increased theta-frequency synchrony between the mPFC and vHPC, as well as theta power in both regions. Notably, mPFC theta power was higher specifically in the "safe" compartments of each arena, decreased immediately prior to entry into the aversive compartments, and correlated with behavioral measures of anxiety. Finally, 5-HT1A KO mice, a genetic model of increased anxiety, had larger mPFC theta power increases than wild type mice. These results further implicate hippocampal theta oscillations in anxiety and suggest that these oscillations may mediate communication between the vHPC and mPFC during exposure to anxiogenic environments.

RESULTS

Neural activity in the medial prefrontal cortex is highly coherent with the ventral but not dorsal hippocampus

To examine the relationship between medial prefrontal cortical and hippocampal activity across the septo-temporal axis of the hippocampus, tungsten microwire electrodes were implanted into the mPFC and the CA1 region of the dHPC and vHPC (Figure S1). For the vHPC electrode, care was taken to ensure placement within the ventral-most third of the hippocampus, as this region in particular has been demonstrated to be crucial for normal anxiety behaviors in lesion studies (Kjelstrup et al., 2002). The mPFC electrode was aimed at the deep layers of the ventral portion of the prelimbic cortex. Following an appropriate recovery period, mice were food

deprived and allowed to forage for pellets in a small rectangular familiar arena. Local field potentials (LFPs) were recorded from each site during daily 10 minute foraging sessions.

As previously described (Buzsaki, 2002), LFPs obtained from the dHPC revealed prominent movement-dependent theta-frequency oscillations (Figure 1). These oscillations were evident both in raw traces (Figure 1A) and in power spectra computed from these traces (Figure 1B). Theta oscillations in the mPFC and vHPC were smaller than in the dHPC (Figure 1B), regardless of hippocampal layer (Figure S2). Nonetheless, activity in the theta range could be measured in vHPC and mPFC power spectra, particularly when the animals were moving at higher speeds.

The similarity of the raw LFP traces from the vHPC and the mPFC (Figure 1A) suggested that the LFPs from these areas might be highly coherent. Indeed, in all animals mPFC-vHPC coherence was high at all frequencies, with peaks in both theta (4-12 Hz) and gamma (30-100 Hz) frequency ranges (Figure 1C). Coherence between dHPC and mPFC was only high for frequencies below 4 Hz, consistent with previous reports that show high synchrony of slow oscillations across the forebrain (Sirota and Buzsaki, 2005). Contamination by motor artifacts may also partially contribute to high coherence at very low frequencies (<1 Hz). Intriguingly, mPFC-vHPC coherence was even higher than coherence between the two hippocampal sites at most frequencies. Notably, dHPC-vHPC coherence was high only in the theta range, and low at gamma frequencies, consistent with similar findings from *in vitro* studies (Gloveli et al., 2005).

High coherence between two LFPs suggests synchronization but does not disambiguate whether the synchrony is due to correlated fluctuations in power (which related to oscillation amplitude) or due to a consistent phase relationship between the two signals (which relates to oscillation timing). To further study coherence between the hippocampus and the mPFC we separately calculated power correlation and phase coherence for theta and gamma frequency ranges. Power correlation was computed by measuring theta and gamma power in each brain area over time throughout the first 10 minutes of each behavioral session. Phase coherence was estimated by computing a histogram of the difference in instantaneous phase across each signal and measuring the width at half height of the histogram peak; narrower peaks indicate a more consistent phase relationship.

For the theta frequency range, both measures revealed stronger synchronization between the mPFC and vHPC than dHPC (Figure 2). The power correlation between mPFC and vHPC was statistically significant for all animals (n=13, $p<0.05$), and the mean r^2 value (0.24) suggests that a considerable portion of the variance in mPFC theta is accounted for by fluctuations in vHPC (or vice-versa). Notably, theta correlations were strongest when the mPFC trace was shifted backwards in time relative to the vHPC (median lag -8 ms, $p<0.05$, signrank test; Figure 4F and G), suggesting the directionality of the relationship is vHPC to mPFC. In contrast to the strong relationship between vHPC and mPFC theta power, weaker correlations were seen between mPFC-dHPC and vHPC- dHPC pairs (n=13, $p<0.05$ for paired t-tests; Figure 2B).

Similarly, theta phase coherence was higher between the mPFC and vHPC than dHPC, as demonstrated by the narrower peak in the phase difference histogram (Figure 2C&D). Surprisingly, vHPC and dHPC showed high theta phase coherence, but low theta power correlation, suggesting that the timing and amplitude of theta oscillations may be influenced by different mechanisms across the dorso-ventral axis of the hippocampus. As expected from the low coherence in the theta range, mPFC and dHPC had low theta power correlations and reasonably independent variation of theta phases, as shown by the wider theta phase difference histogram (Figure 2C&D).

In addition to high theta range coherence, LFPs from the mPFC and vHPC also had high gamma coherence. We therefore also examined power correlations and phase coherence of gamma-frequency oscillations. Even though gamma oscillations are thought to be generated locally, power correlations in the gamma range were higher for mPFC-vHPC than for mPFC-dHPC or dHPC-vHPC (n=13, p<0.01 for each paired t-test; Figure 2B). Similar to theta phase coherence, gamma phase coherence was moderately high between mPFC-vHPC and dHPC-vHPC electrode pairs (Figure S3 panel B).

To further study hippocampal-mPFC interactions we also investigated whether hippocampal theta phase influences mPFC gamma power. In the dHPC, gamma power is modulated by local theta phase, (Buzsaki et al., 2003; Csicsvari et al., 2003) presumably because the activity of interneurons that give rise to dHPC gamma is modulated by the theta oscillation. If the vHPC projections to the mPFC oscillate at theta and influence the activity of mPFC interneurons that generate gamma (Szabadics et al., 2001; Tierney et al., 2004), vHPC theta phase may be expected to modulate mPFC gamma power, as shown previously for the dHPC (Sirota et al., 2008). Indeed, mPFC gamma power was more strongly modulated by vHPC theta than dHPC theta (Figure S4).

Theta power correlations between the mPFC and vHPC increase in the EPM and the open field

Since the mPFC and vHPC are likely involved in the regulation of anxiety-like behavior, we examined whether the synchronization between these areas was modulated during exposure to anxiogenic environments. Following testing in the familiar arena, mice were exposed to a novel open field and an EPM, in counterbalanced order with two intervening rest days. Results from each anxiety paradigm were compared to the recordings obtained from the familiar environment on the same day. Percent time spent, and path length in the center of the open field, as well as percent time spent and entries into the open arms of the EPM, were used as pharmacologically validated measures of anxiety-like behavior (Choleris et al., 2001; Lister, 1987). Mice demonstrated a variable anxiety-like response to the two environments, ranging from complete avoidance to robust exploration of the aversive parts of each arena (Figure S7). Measures of anxiety-like behavior correlated well across the two tests, suggesting that both measured similar anxiety-like traits (see Methods).

During these exposures to the EPM and open field, raw LFP traces from the mPFC displayed more robust and regular theta oscillations compared to the familiar arena (Figure 5A). The higher prominence of theta in the raw traces suggested that theta-range synchrony between the vHPC and mPFC might be increased. Indeed, we found increases in theta-frequency power correlations between the vHPC and the mPFC in the open field compared to the familiar arena (n=11, p<0.04 for a paired t-test) (Figure 3C). Similar results were found in the EPM (n=11, p<0.01 for a paired t-test), supporting the idea that theta synchrony between the mPFC and vHPC increases during exposure to these environments (Figure 3D). Moreover, the increase in power correlation was specific to the theta range and to the mPFC-vHPC pair (Figure 3C and D and S3). Power correlations with the dHPC did not change in any of the anxiety paradigms. Peak mPFC theta frequency increased to nearly 8 Hz in the EPM and the open field, becoming closer to vHPC theta frequency (Figure S3 panel D), consistent with increased synchrony between these two regions. This pattern of results was observed in all HPC layers (Figure S2) and was present in all compartments of both the EPM and the open field (Figure S3, panels E and F). Other measures of synchrony did not change significantly in either test (Figure S3).

Phase-locking of mPFC neurons to local and vHPC theta oscillations increases in the open field

The above data obtained from LFPs suggest that theta synchrony between the mPFC and vHPC increases in the open field and the EPM. However, the anatomical origins of LFPs may be unclear due to possible contamination by volume-conducted signals from more distant sites, or signals in the reference wire. By contrast, spiking activity is not subject to either artifact. To confirm the observed increases in mPFC-vHPC theta synchrony, we measured the phase-locking of mPFC multiunit spiking activity to local and hippocampal theta during exposure to the familiar environment and the open field. The magnitude of phase-locking was measured using the mean resultant length (MRL), a measure of circular concentration derived from Rayleigh's test of circular uniformity (see Experimental Procedures). By this measure, the open field led to increases in phase-locking to both mPFC and vHPC, but not dHPC theta oscillations (Figure 4B).

Analysis of phase locking of mPFC spikes to hippocampal theta also permits confirmation of the directionality of the functional connectivity between the vHPC and mPFC. To address this issue, phase locking of multiunit activity was calculated after shifting the spikes forward and backward in time relative to the LFP. If mPFC cells are influenced by the hippocampal field, phase locking should be maximal when spikes are shifted backwards (i.e., negative temporal offsets in Figure 4C-E). Interestingly, this analysis shows that on average mPFC spikes were maximally phase locked to hippocampal theta of the past (Figure. 4D and E), both for vHPC (mean shift=−32 ms, n=30 recordings, p<0.01, Wilcoxon's signed rank test) and dHPC theta oscillations (mean shift=−36 ms, n=30 recordings, p<0.03, Wilcoxon's signed rank test). Reports of a similar analysis performed in rats for dHPC theta and mPFC spikes found a mean shift of −45 ms, in broad agreement with the present results (Siapas et al., 2005). These shifts are also generally consistent with delays of antidromic spikes (16 ms) between the ventral hippocampus and mPFC taking into account polysynaptic connectivity (Thierry et al., 2000), and confirm the directionality suggested by the analysis of theta power correlation in the LFPs (Figure 4G). Furthermore, as expected, mPFC spikes are maximally phase locked to local theta oscillations at a temporal offset close to zero (mean shift=1.7 ms, n=28 recordings), suggesting that theta recorded in the mPFC has immediate local relevance. These results are consistent with the notion that theta-frequency input to the mPFC from the ventral hippocampus modulates mPFC unit activity, and the strength of this modulation is increased during exploration of anxiety-provoking environments.

Theta power in the mPFC and vHPC increases in the open field and the EPM

Consistent with our observations from the raw LFP traces, we found that theta power increased in the vHPC and the mPFC in both anxiety tests (Figure 5). To reliably measure low values of theta power, we fit all spectra with the sum of an exponential and a Gaussian curve, the latter centered at theta frequency (see Experimental Procedures). The area under the Gaussian was used as a measure of total theta power. The finding that theta power increases with higher speeds (Figure 1) shows that theta power can be modulated by behavioral variables other than anxiety. Thus, comparisons of power across environments were done during epochs of similar movement (7-15 cm/s, unless otherwise stated). In the vHPC, but not the dHPC, theta power was higher in both the open field and the elevated plus maze relative to the familiar arena (Figure 5C, n=11, p<0.05 in a paired Wilcoxon's signed rank test). In the mPFC, theta power also increased in the open field (Figure 5C, n=18, p<0.05 for a paired Wilcoxon's signed rank test), although the increase did not reach statistical significance in the EPM (Figure 5C, n = 12, p = 0.3). Importantly, these results cannot be explained by novelty, because theta power in the mPFC and vHPC in the anxiogenic environments was also increased relative to the first day of exposure to the then-novel "familiar" arena (Figure 5C, right panel). These results were

consistent across all hippocampal layers (Figure S2) and could not be explained by differences in speed or acceleration (Figure S5).

To better define the behavioral relevance of these increases in theta power, we separately compared theta power in each compartment of the open field and EPM to that in the familiar arena (Figure 6A&B). The observed increases in vHPC theta power were present in both the center and periphery of the open field, and in all three compartments of the EPM (open arms, closed arms and center). Intriguingly, theta power in the mPFC was significantly modulated by location within each environment; mPFC theta power was increased only in the relatively protected periphery of the open field and closed arms of the EPM.

These results suggest the possibility that theta-frequency activity in the mPFC reflects a role for the structure in inhibiting the active exploration of the aversive areas within each environment. To further explore this possibility, we examined the temporal dynamics of mPFC theta power in the EPM, where transitions between compartments could be precisely identified based on the animal's location. Spectrograms of mPFC field potentials were calculated centered on the transition point when the animal passed from the closed arm into the center of the EPM. The averaged spectrogram of all such transitions (Figure 7A) shows a dramatic decline in mPFC theta power 2-3 seconds *before* the animal leaves the closed arm. mPFC theta power also increased before the reverse, center-to-closed arm transitions (Figure 7B). Notably, mPFC-vHPC coherence showed a similar pattern, decreasing before the animal leaves the closed arms (Figure 7 C and D). The timing of these changes suggests the possibility that theta-frequency activity in the mPFC is involved in actively inhibiting exploratory behavior, rather than simply reflecting the position of the animal with the maze. Importantly, there are no overt changes in locomotor behavior during transitions that could account for these results (Figure 7 E-G).

To further characterize the behavioral role of mPFC theta activity, we directly examined the relationship between the increase in mPFC theta power and anxiety-related behavior in each test across animals. In both the open field (Figure 8A) and the EPM (Figure 8B) there was a significant correlation between the magnitude of the increase in mPFC theta power and anxiety-related behavioral measures. Animals with the largest increases in theta power spent the least time in the center of the open field, or in the open arms of the EPM. The relationship between theta and behavior held even when considering only the magnitude of the increase only in the periphery of the open field (Figure 8C) or the closed arms of the EPM (Figure 8D). These data further support the hypothesis that that increases in mPFC theta power are associated directly with anxiety-like behavior.

Serotonin 1A receptor knockout mice have higher increases in mPFC theta power with anxiety

Serotonin 1A receptor (5-HT1AR) knockout mice display increased anxiety-like behavior relative to wild-type animals in hippocampal-dependent anxiety tests, including the EPM and the open field (Ramboz et al., 1998). 5-HT1AR knockout mice also were shown to have increased theta power in the pyramidal layer of the dHPC in the EPM relative to a control environment (Gordon et al., 2005). Considering that our data show increased theta power in the EPM and in the open field in the vHPC and the mPFC in wildtype mice, we hypothesized that the more anxious 5-HT1A knockout mice would have a larger increase in theta power during exploration of the EPM and open field. 5-HT1AR knockouts and wildtype littermates underwent electrode implantation and were tested in familiar, EPM and open field environments. In knockouts, as in wildtypes, the mPFC was more tightly coupled to the vHPC than the dHPC in the familiar environment (data not shown). In both the EPM and open field, however, knockouts had a larger increase in mPFC theta power than their wildtype littermates (Figure 9A and B, n= 7 WT and 7 5-HT1A KO mice, p<0.04). The fold increase in mPFC theta

power in 5-HT1A knockouts was also significantly greater than that of the pooled group of all wildtype mice. The theta power increase in the vHPC was not statistically different from that of the wildtypes in our small sample. We also did not find significant theta power increases in the dHPC of 5-HT1A knockouts, contrary to that found in the pyramidal layer of the dHPC in our previous report (Gordon et al., 2005),perhaps due to the smaller sample size or decreased anxiogenicity of the EPM in the current study. It should be noted that the 95% confidence interval for the dHPC increase seen in the current study (1.03 fold ± 0.33) overlaps with the fold increase reported in the previous study (1.2).

DISCUSSION

While a role for the vHPC in anxiety has been clearly established (Bannerman et al., 2004; Kjelstrup et al., 2002), the mechanism by which the vHPC exerts its anxiogenic effect has not been previously explored. Here, for the first time, we demonstrate theta-frequency synchronization between the vHPC and a principal downstream target, the mPFC. At baseline, this synchronization is significantly larger than that between the dHPC and mPFC. Anxiety further enhances the strength of vHPC-mPFC synchrony without affecting mPFC-dHPC synchrony, as found with both multiunit and LFP data. Accompanying this increase in synchrony is an increase in theta-frequency activity in the mPFC that appears to be involved in inhibition of exploratory behavior. These results are consistent with the known anatomical relationship between the hippocampus and the mPFC, and indicate that the vHPC and mPFC may act together to generate behavioral inhibition during anxiety tests.

Functional connectivity between the hippocampus and the mPFC

Previous studies have demonstrated that neural activity in the mPFC synchronizes with theta-frequency oscillations in the dHPC (Hyman et al., 2005; Jones and Wilson, 2005) despite the fact that these two regions are indirectly connected (Burwell R.D. and Witter, 2002); (Hoover and Vertes, 2007). In contrast, the vHPC and the mPFC are directly connected (Hoover and Vertes, 2007; Parent et al., 2009; Thierry et al., 2000; Verwer et al., 1997). However, no previous attempts have been made to measure functional coupling between these two structures. Here we find that the mPFC is more highly coherent with the vHPC than the dHPC, over a broad range of frequencies, though only theta-range synchrony was modulated by anxiety. Further studies are needed to investigate if mPFC-vHPC synchrony in other frequency ranges is modulated by different tasks. It is noteworthy that previous HPC-mPFC anatomy work shows that mid HPC, (mHPC), also projects to mPFC, although less robustly than the vHPC (Hoover and Vertes, 2007). In agreement with these reports, recordings performed in mHPC displayed theta-range coherence and anxiety-induced changes in theta power that are in between those of dHPC and vHPC (Figure S6).

A higher degree of coupling between the mPFC and vHPC was also reflected in other measures, such as gamma-frequency coherence, and modulation of mPFC gamma power by hippocampal theta phase. Finally, theta-frequency synchronization between the vHPC and mPFC increased in anxiogenic environments. Taken together, these data strongly argue that the vHPC-mPFC functional connection is an important one.

An interesting finding with functional implications is that the vHPC has high theta-frequency coherence with both the dHPC and mPFC, despite low dHPC-mPFC coherence. This seemingly paradoxical result is possible because vHPC-mPFC and vHPC-dHPC theta coherence may occur at different times or in different theta sub-frequencies (see example in Figure S7, panel A). Furthermore, measurements of vHPC-dHPC and vHPC-mPFC theta coherence over time seem to be negatively correlated (Figure S7, panel B). These findings argue that while theta generators in the dHPC and vHPC are synchronized, they are nonetheless somewhat independent, possibly subserving different behavioral functions. Perhaps the vHPC might

synchronize with the dHPC to process spatial information, while it synchronizes with the mPFC to modulate anxiety-related behaviors.

Such interpretations must, however, be tempered by the caveats inherent in experiments relying on LFPs. Although LFPs reflect the activity of large groups of synapses, allowing analysis of synchronous activity within and across areas, the anatomical origins of LFPs can sometimes be questionable. Recorded voltage fluctuations can arise from volume conduction of distant signals. Several of our findings suggest that it is unlikely that volume conduction accounts for a substantial fraction of the theta-frequency coherence seen in our recordings. First, we found mPFC-vHPC coherence to be higher than mPFC-dHPC coherence, despite the fact that the mPFC is much further from vHPC (5.9 mm) than dHPC (3.7 mm). Since volume-conducted signals reflect distance rather than anatomical connectivity, coherence between more distant areas would be smaller, rather than larger, if accounted for by volume conduction. Second, we found that multiunit activity in the mPFC, which is not subject to volume conduction artifacts, phase-locks more robustly to local and vHPC theta, but not dHPC theta, during exploration of the open field. Third, in the familiar environment theta oscillations in the mPFC and in the hippocampus occur at different frequencies (Figure S3, panel D). Cortical and hippocampal oscillations would have the same frequency if they were volume conducted from the hippocampus. These results argue strongly that the synchrony described is not due to volume conduction of signals into the mPFC from elsewhere. Finally, to show that our vHPC field potential recordings have local relevance, we show that multiunit activity recorded in the vHPC is phase locked both to local theta and gamma oscillations (Figure S8).

Another possible source of artifacts in field potential analysis is contamination of the LFP by oscillations recorded not in the brain area of interest, but in the reference electrode. In order to rule out this possibility we demonstrate that the vHPC LFP traces are similar when recorded against the frontal reference or the posterior ground screw (Figure S8), and that each of the main findings can be reproduced using the ground screw as an alternate reference (Figure S9). Furthermore, spikes in the mPFC were found to be maximally phase-locked to the simultaneously occurring mPFC theta, while phase locking to vHPC and dHPC theta was strongest after a lag of tens of milliseconds, consistent with previously reported delays for this pathway (Thierry et al., 2000). If a substantial amount of vHPC and mPFC theta oscillations were due to contamination from the reference this result would not be possible, as spikes would be expected to phase lock maximally to both vHPC and mPFC theta with a similar temporal offset. These analyses strongly support the notion that increases in vHPC-mPFC synchrony reflect hippocampal influences on local neuronal activity within the mPFC.

mPFC and vHPC in anxiety

Previous work has shown that lesions of the vHPC (Bannerman et al., 2004; Kjelstrup et al., 2002) or mPFC (Gonzalez et al., 2000; Lacroix et al., 2000; Shah and Treit, 2003) decrease anxiety-related behaviors in anxiety tests. The current study is the first to record neural activity from these areas in anxiogenic environments. Our data demonstrate that mPFC-vHPC theta-frequency synchrony is increased in anxiety tests, as shown by both LFP and multiunit data, suggesting that these areas cooperate to modulate anxiety. Furthermore, mPFC spikes were found to be optimally phase locked to HPC theta oscillations of the past, and crosscorrelations of mPFC and vHPC theta power peaked at a negative lag, consistent with the hypothesis that theta range activity is propagated from the vHPC to the mPFC.

Recent experiments showing a role for the vHPC in spatial representation (Kjelstrup et al., 2008) suggest how the vHPC might act in anxiety. The role of the hippocampus in contextual representation has been studied extensively in the dHPC, where place-selective cells provide fine-scale spatial information. A recent report has shown that the vHPC also has place cells, but with much larger place fields than dHPC cells (Kjelstrup et al., 2008). Larger place fields

may be well suited to guide emotional behavior, because generally the stimuli involved in anxiety tests are less spatially discrete. Thus it may be that the vHPC provides contextual (or other larger-scale spatiotemporal) information to downstream structures such as the mPFC, where the decision to engage in defensive vs. exploratory behaviors may be made, perhaps by modulating activity in downstream structures such as the amygdala.

The known anatomical and functional characteristics of the mPFC are consistent with the notion that it interprets contextual information to influence the expression of anxiety-like behaviors. The mPFC receives projections not only from the vHPC but also from multi modal association cortices and the rhinal cortices (Hoover and Vertes, 2007), giving it access to highly processed information about the environment. The mPFC then projects directly to structures such as the amygdala and the periaqueductal grey (Vertes, 2004), which can act to produce appropriate defensive behaviors. Stimulation of the prelimbic cortex decreases recall of fear extinction, consistent with the idea that this subregion of the mPFC acts to increase anxiety-like behaviors (Vidal-Gonzalez et al., 2006). The mPFC recordings reported here were from the deep layers of the prelimbic cortex, suggesting that the physiological differences found in the mPFC in the EPM and open field may have an anxiogenic role.

The specificity of the increase in theta power in the mPFC is intriguing from a mechanistic and functional standpoint. The high theta coherence throughout the anxiety-provoking environment suggests that coordination of vHPC-mPFC activity is uniformly expressed. The selective increase in theta power in the "safe" aspects of each environment raises the possibility that a change intrinsic to the mPFC increases the gain of this functional connection. Functionally, the spatial distribution and dynamics of the theta power increase are consistent with a role for mPFC theta in inhibition of exploratory behavior during anxiety. A role for the mPFC in behavioral inhibition is in line with prior work, such as reports of higher aggressiveness in rats with lower levels of mPFC GABA (Sustkova-Fiserova et al., 2009). Involvement of the mPFC in behavioral inhibition has also been found in attention tasks, such as the 5-choice serial reaction time task, where higher levels of the serotonin metabolite 5-hydrohyindoleacetic acid in the mPFC were found to correlate with impulsive and premature choices (Puumala and Sirvio, 1998). Furthermore, cytotoxic lesions of the mPFC have been shown to decrease prepulse inhibition and induce hyperlocomotion (Yee, 2000). Lastly, various studies have showed that mPFC lesions decrease fear and anxiety -related responses, both in tasks that depend on the vHPC, such as the EPM (Shah and Treit, 2003, 2004), and paradigms that do not require the vHPC, such as extinction of conditioned fear (Burgos-Robles et al., 2007) and the Vogel conflict test (Resstel et al., 2008). Thus, diverse studies using different behavioral paradigms support a role for the mPFC in behavioral inhibition, consistent with the present work.

The data obtained from the 5-HT1AR knockouts are consistent with the hypothesis that both the vHPC and mPFC have a role in the generation of anxiety. A role for the hippocampus in their anxiety phenotype has already been hypothesized based on several factors: hippocampal 5-HT1A receptors have been shown to modulate anxiety (File et al., 1996); 5HT1AR knockout mice are specifically more anxious only in paradigms which require the hippocampus (Gordon et al., 2005; Klemenhagen et al., 2006); restoring forebrain expression of the receptor rescues the anxiety phenotype (Gross et al., 2002); and the elevated plus maze induces an increase in theta power in the knockouts (Gordon et al., 2005). Here we report a larger anxiety-induced increase in mPFC theta power in the knockouts. While these results do not resolve whether the primary alteration in 5-HT1AR knockouts resides in hippocampal hyperactivity or in the ability of the vHPC and mPFC to synchronize, they lend further credence to the hypothesis that the increases in mPFC theta power seen in the wild-types are indeed due to anxiety rather than unrelated behavioral effects of the open field and EPM.

While theta-frequency oscillations are prominently featured in the data supporting the current model, their importance is debatable. On one hand, we present data from two different anxiety tests linking the strength of theta oscillations in the mPFC with behavioral measures of anxiety. These data are consistent with existing hypotheses suggesting a specific role for hippocampal theta oscillations in behavioral inhibition and hippocampal-dependent anxiety (McNaughton and Gray, 2000). On the other hand, we cannot rule out the possibility that anxiety may require only that the vHPC communicates with the mPFC, and not that it uses theta oscillations to do so. Experiments aimed at perturbing theta generation by pharmacological or genetic manipulations are necessary to elucidate this question. In any case, our data suggests that the vHPC-mPFC connection is important for the modulation of anxiety-related behavior.

CONCLUSION

The present results show that theta range synchrony between the vHPC and the mPFC is modulated by anxiety. This finding suggests a model in which the vHPC sends the mPFC large-scale information about the emotional salience of the environment, which allows the mPFC to recognize the environment as threatening. The mPFC may in turn modulate the amygdala to produce appropriate defensive and anxiety-related behaviors. Importantly, behavioral modulation of theta synchrony has been shown previously between the dHPC and other structures such as the amygdala in fear conditioning (Seidenbecher et al., 2003), the striatum in learning (DeCoteau et al., 2007), and the mPFC in working memory (Jones and Wilson, 2005). Together these studies are consistent with the emerging notion that theta range synchronization between the hippocampus and other areas is a general mechanism by which information is transmitted between the hippocampus and downstream structures relevant to ongoing behavior.

EXPERIMENTAL PROCEDURES

Animals

Three to six month old male wildtype 129Sv/Ev mice were obtained from Taconic (Germantown, NY, USA). 5-HT1AR knock-out mice and littermate controls were generated from heterozygote breeding pairs on a 129SvEv background as described previously (Ramboz et al., 1998). Eighteen wild type and seven 5-HT1AR knockout mice were used for the simultaneous mPFC, dHPC and vHPC recordings. An additional two wild-type mice were used for the ventral hippocampus multiunit recordings. Experiments comparing knockouts and wild-types were conducted blind to genotype. The procedures described here were conducted in accordance with National Institutes of Health regulations and approved by the Columbia University and New York State Psychiatric Institute Institutional Animal Care and Use Committees.

Microdrive Construction

Custom microdrives were constructed using interface boards (EIB-16, Neuralynx, Bozeman MT) fastened to a Teflon platform. This platform was fastened to Teflon cuffs via fine machine screws (SHCX-080-6, Small Parts, Inc, Miramar, FL), permitting the platform to advance by turning the screws into the cuffs. Electrodes were made from Formvar-coated tungsten microwire (California Fine Wire, Grover Beach, CA). The mPFC electrodes were fastened to a cannula attached to the platform to permit them to be lowered precisely after implantation; hippocampal electrodes were stereotactically placed and cemented directly to the skull during surgery.

Surgery

Animals were deeply anesthetized with ketamine and xylazine (165 and 5.5 mg/kg, in saline) and supplemented with inhaled isoflurane (0.5-1%) in oxygen. Mice rested on a heating pad regulated by a feedback controller; temperature was monitored with a rectal probe. Mice were secured in a stereotactic apparatus (Kopf Instruments, Tujunga, CA) and the skull was leveled using bregma and lambda landmarks. Screws were implanted on the posterior and anterior portions of the skull to serve as ground and reference, respectively. Anterior-posterior and medial-lateral coordinates were measured from bregma, while depth was calculated relative to brain surface. Tungsten wire electrodes were implanted through burr holes targeting the following locations: dHPC CA1 (1.94 mm posterior, 1.5 mm lateral and 1.4 mm depth), vHPC CA1 (3.16 mm posterior, 3.0 mm lateral and 4.2 mm depth) and mPFC (+1.65 mm anterior, 0.5 mm lateral and 1.5 mm depth). These coordinates resulted in electrode tips located near the fissure or in the stratum lacunosum-moleculare for the hippocampal electrodes, and in the deep layers of the ventral portion of the prelimbic cortex for the mPFC electrodes. Electrodes were implanted at the vHPC and dHPC sites and cemented directly to the skull with Grip Dental Cement (Dentsply, Milford, DE). The microdrive was then placed carefully over the skull with a micromanipulator, and the attached mPFC electrode was lowered to the appropriate depth. The Teflon cuffs were then cemented to the skull, and the ground and reference screws as well as the hippocampal electrodes were connected to the interface board. Lastly, walls of dental cement were built between adjacent cuffs to protect the electrodes from external debris. Animals were monitored postoperatively and given analgesics (Carprofen, 5 mg/kg S.C.) as necessary. Following surgery, animals were housed individually with bedding squares provided for enrichment.

Behavioral Protocol

Animals were permitted to recover for at least one week or until regaining pre-surgery body weight. Mice were then food restricted to 85% body weight. During food restriction animals were familiarized to the recording setup and handling by being tethered to the head stage preamplifier in their home cages for 5-7 daily sessions of 20 minutes each. Upon reaching their target weight, mice were exposed to a small rectangular box ("familiar arena", 30×20 cm) in the dark in which they foraged for pellets for 4 or more daily sessions of 10 minutes. Twelve wild type and seven 5HT1AR knockout mice were exposed to either the open field or the EPM for 10 minutes following a one hour resting period after the exposure to this familiar arena. After 2 days of rest the procedure was repeated with the other anxiogenic environment. The order of presentation of the two environments was counterbalanced across animals. Additionally, a group of 6 wild-type mice were exposed only to the open field. Physiological and behavioral measures did not vary across groups. Wild type mice spent 53% of the time in the open arms of the EPM and 15% of the time in the center of the open field. The EPM and the open field were found to be anxiogenic in both wild type and 5HT1AR knockout mice. However, we were unable to detect differences between the two genotypes in classical behavioral measures of anxiety in the current cohort, likely because it was too small; group sizes of 20-25 animals are typically required to detect behavioral differences between knockouts and wildtypes in these tests (Ramboz et al., 1998). Nevertheless, we found expected differences in total path length in the open field (1061±79 and 851±83, for WTs and KOs, respectively), consistent with previous reports (Gross et al., 2002). Decreased total path length is indicative of increased responsiveness to the anxiogenic environment in the knockout mice and higher behavioral inhibition.

Exposures to the EPM were done at 200 lux. The elevated plus maze was constructed of wood painted grey and consisted of four arms, 7.6 cm wide and 28 cm long, elevated 31 cm above the floor. Two opposing arms were enclosed by 15-cm-high walls, whereas two were open except for a 1-cm-high lip at the edge. The open field consisted of a wooden round grey circular

arena with 25 cm radius and 40 cm height. In order to permit a better behavior/physiology correlation, it was necessary to increase the variance in center time by altering the illumination in the open field. Therefore, half of the open field recordings were done at 20 lux, while the other half was done at 120 lux. As intended, recordings done at 20 lux increased exploration of center of the open field, and diminished the fold increase of theta power in the mPFC (1.41 ±0.1 and 1.0±0.13, for 120 and 20 lux, respectively). The finding that light levels affected center time (9.1±6 and 30.7±15, for 120 and 20 lux, respectively), as previously shown (Barrot et al., 2002), strongly suggests that % time spent in the center of the open field is a valid measure of anxiety in the current cohort. Comparisons between wildtype and 5-HT1AR knockout mice were done at 20 lux. All the other analyses pooled the results from both 20 and 120 lux recordings.

The open field was clearly anxiogenic in our cohort, as the majority of mice spent less than 10% of the time exploring the brightly lit center of the open field (Figure 8A), in line with previous behavioral reports in mice (Fee et al., 2004) and in rats (Cannizzaro et al., 2003). Not all mice displayed robust avoidance of the open arms in the EPM. However, mice that displayed high anxiety in the EPM also did the same in the open field. Accordingly, % time spent in the center of the open field and % time spent in the open arms of the EPM were significantly correlated (r=0.48, p=0.04). This suggests that these measures are associated with individual trait-level anxiety. Moreover, % time spent in open arms was highly correlated across multiple exposures to the EPM in a subset of the animals exposed to the EPM twice (r=0.8, p=0.01). These results are consistent with the notion that the behavioral measures used in the current work reflect trait-anxiety. Although some animals were exposed to the EPM for two days, neural data from the second exposure was not analyzed.

In order to verify whether vHPC field potentials have local relevance, two mice were implanted with electrodes in the following coordinates targeting the vHPC: 3.16 mm posterior, 3.0 mm lateral and 3.2 mm depth. Electrodes were lowered across days until a dramatic increase in multiunit activity was found. The electrodes were judged to have reached the pyramidal layer in that day. Data from figure S8 is from a session in the familiar environment after the pyramidal layer was reached. At the end of the experiment mice were sacrificed and perfused transcardially. Electrode position was subsequently confirmed with Nissl staining.

Data Acquisition

Recordings were obtained via a unitary gain head-stage preamplifier (HS-16; Neuralynx) attached to a fine wire cable suspended on a pulley so as not to add any weight to the animal's head. LFPs were recorded against the reference screw located above the olfactory bulb. Field potential signals were amplified, bandpass filtered (1-1000 Hz) and acquired at 1893 Hz. Multiunit activity from mPFC was recorded simultaneously from the same electrodes used to obtain LFPs; multiunit signals were bandpass filtered (600-6000 Hz) and recorded at 32 kHz. Spikes exceeding a threshold of 400 μV were selected for analysis of phase-locking to theta (see below). Both LFP and multiunit data were acquired by a Lynx 8 programmable amplifier (Neuralynx) on a personal computer running Cheetah data acquisition software (Neuralynx). The animal's position was obtained by overhead video tracking (30 Hz) of two light-emitting diodes affixed to the head stage.

Data Analysis

Data was imported into Matlab for analysis using custom-written software. Velocity was calculated from position records and smoothed using a window of 0.33 seconds. Measurements that were found to be affected by speed, such as coherence and power spectra, were calculated from data acquired during segments of consistent movement between 7-15 cm/s. The results described were not affected by the specific speed range used. Spectral analysis of LFPs were

done using Matlab's signal processing toolbox functions along with custom software. Power spectra were calculated using the Welch method with a moving window of 0.4 s, with 90% overlap, and 4000 nFFTs. Coherence was calculated with the multitaper method, using a time-bandwidth product of 30. Confidence intervals were calculated through a jackknife method across animals and tapers. These specific parameters were optimized empirically but the results were robust to changes in any given parameter. Coherence at very high frequencies (>100 Hz) was high between all brain areas. This is likely because biological oscillations in this frequency range are small relative to noise common to all recording sites under our recording conditions.

In order to calculate theta power accurately, we fitted power spectra with the sum of an exponential and a Gaussian using Matlab's cfit function from the curve fitting tool box. The area of the theta-centered Gaussian was taken as the measure of theta power. Unless otherwise stated all power spectra, coherence plots and fold power increases bar graphs shown in figures and Supplemental Data figures are from data collected while animals were moving between 7 and 15 cm/s.

Coherence is comprised of power correlations and consistency of phase (phase coherence). We analyzed these two measures separately for they may vary independently. To calculate power correlations across areas, theta and gamma power were calculated over time. Individual points in the power correlation plots (Figure 3A) represent average theta power calculated through a multitaper spectrogram method with an NW of 2.5. A window size of 5000 samples (2.6 seconds) with no overlap between successive windows across 10 minutes of recording was used. The linear correlation coefficient for each plot was calculated and averaged across animals for each pair of brain areas. Fisher's Z-transform was calculated on the correlation coefficients to obtain a normally distributed population of values. Student's t-tests were then performed to compare the transformed r values for mPFC-dHPC and mPFC-vHPC. Power correlations, as well as theta phase difference histograms were calculated on data from the entire recording, regardless of the speed of the animal. The consistency of the phase relationship was measured by calculating the instantaneous theta phases of two signals through the Hilbert transform and then subtracting the phases of the 2 LFPs from each other. Only time points during which hippocampal theta power was greater than the mean theta power for that session were used. The phase differences obtained were then plotted as histograms, and the width of this plot at half of the peak height was used as a measure of the consistency of the phase relationship of the two signals. If two signals tend to have a constant phase relationship (i.e., the difference between the phases of the two signals tends to be constant), the phase difference histogram will display a narrow peak, independent of the absolute mean phase difference.

To measure the influence of hippocampal theta phase on mPFC gamma power, instantaneous values for theta phase and gamma amplitude were obtained using a Hilbert transform on band-pass filtered LFP data. The strength of the modulation of gamma amplitude by theta phase was measured by first normalizing to the mean gamma power and then computing the fractional modulation of gamma amplitude by theta phase.

The strength of multiunit phase-locking to theta oscillations was assessed by comparing the mean resultant length vector (MRL), which is derived from Rayleigh's z statistic of circular uniformity across environments. Only data obtained while animals were moving (velocity > 4 cm/s) were used to compute phase-locking for theta because theta power is low during immobility, preventing accurate estimation of theta phase. To determine whether spikes were phase-locked to theta, theta phases of LFPs were determined through the Hilbert transform, and a phase was assigned to each spike based on the time of the spike's occurrence. A phase of 0 refers to the trough of the theta cycle as recorded. The magnitude of phase-locking can be measured through Rayleigh's z parameter. MRL (MRL=(z/number of spikes)$^{0.5}$) was used in comparisons instead of z because the population of MRL values has a lower variance than the

z population. Higher modulation of firing by theta phase increases MRL. However, it is important to note that high MRL values can also be obtained by calculating Rayleigh's statistic on a sample with few spikes, thus only recordings with a minimum of 700 spikes in both environments were analyzed. To avoid changes in MRL due to fluctuations in firing rate, the same number of spikes was analyzed in a given multiunit recording across environments. A paired Wilcoxon's test on MRL values was used to determine if phase-locking of multiunit activity to mPFC, dHPC and vHPC theta increased in the open field relative to the familiar arena. To determine the temporal relationship between multiunit activity and theta oscillations in each area, phase locking was calculated for 40 different temporal offsets for each multiunit recording. Units with significant Bonferroni-corrected phase locking in at least one of the 40 shifts were used for the analysis in Figure 4 C-E.

In order to calculate changes in mPFC theta power during transitions from the closed arm to the center, spectrograms spanning 10 seconds centered at the transitions were calculated. The multitaper method was used, with 20000 nFFTs, in 2-second windows with 97% overlap, 1.5 NW and 5 tapers. Spectrograms of all transitions in all mice were averaged and plotted on Figure 7. For closed-center transitions, the open and center compartments were treated as one compartment. This was done as both the open arms and the center are anxiogenic compartments, with similar changes in theta power (Figure 7). Coherograms centered at the transitions were calculated with 0.5-second windows with 0.3-second overlap and 3700 nFFTs. These coherence values are not directly comparable to the ones shown in Figure 1C, as the parameters used for the estimation of coherence were different.

Statistics

Paired Wilcoxon's signed rank tests were used for comparisons involving measurements from the same animal across behavioral conditions, such as changes in theta power in anxiogenic environments relative to the familiar arena. Comparisons between populations of r^2 across environment or across brain areas were performed with paired t-tests on the Fisher's Z transformed r values. The use of t-tests in this case is warranted because the Z transform produces a normal distribution, as verified through the Lilliefors test for normality. Standard error of means (S.E.Ms) were plotted in bar graphs to show the accuracy of the estimation of the mean of the population. Two-tailed tests were used throughout.

Histology and Genotype Confirmation

Upon the completion of recording, animals were deeply anesthetized and electrolytic lesions were made to determine the position of the electrode tips. Lastly, animals were tail clipped and perfused with formalin. Brain sections were mounted on slides to visualize and photograph lesions. For 5-HT1AR knockouts and control littermates, DNA was extracted from the clipped tails to reconfirm genotype through PCR.

Supplementary Material

Refer to Web version on PubMed Central for supplementary material.

Acknowledgments

REFERENCES

Bannerman DM, Rawlins JN, McHugh SB, Deacon RM, Yee BK, Bast T, Zhang WN, Pothuizen HH, Feldon J. Regional dissociations within the hippocampus--memory and anxiety. Neurosci Biobehav Rev 2004;28:273–283. [PubMed: 15225971]

Barrot M, Olivier JD, Perrotti LI, DiLeone RJ, Berton O, Eisch AJ, Impey S, Storm DR, Neve RL, Yin JC, et al. CREB activity in the nucleus accumbens shell controls gating of behavioral responses to emotional stimuli. Proc Natl Acad Sci U S A 2002;99:11435–11440. [PubMed: 12165570]

Burgos-Robles A, Vidal-Gonzalez I, Santini E, Quirk GJ. Consolidation of fear extinction requires NMDA receptor-dependent bursting in the ventromedial prefrontal cortex. Neuron 2007;53:871–880. [PubMed: 17359921]

Burwell, RD.; Witter, MP. Basic anatomy of the parahippocampal region in monkeys and rats. Oxford University Press; New York: 2002.

Buzsaki G. Theta oscillations in the hippocampus. Neuron 2002;33:325–340. [PubMed: 11832222]

Buzsaki G, Buhl DL, Harris KD, Csicsvari J, Czeh B, Morozov A. Hippocampal network patterns of activity in the mouse. Neuroscience 2003;116:201–211. [PubMed: 12535953]

Cannizzaro C, Martire M, Cannizzaro E, Monastero R, Gagliano M, Mineo A, Provenzano G. Effects of 8-OH-DPAT on open field performance of young and aged rats prenatally exposed to diazepam: a tool to reveal 5-HT1A receptor function. Eur Neuropsychopharmacol 2003;13:209–217. [PubMed: 12729947]

Choleris E, Thomas AW, Kavaliers M, Prato FS. A detailed ethological analysis of the mouse open field test: effects of diazepam, chlordiazepoxide and an extremely low frequency pulsed magnetic field. Neurosci Biobehav Rev 2001;25:235–260. [PubMed: 11378179]

Corcoran KA, Quirk GJ. Activity in prelimbic cortex is necessary for the expression of learned, but not innate, fears. J Neurosci 2007;27:840–844. [PubMed: 17251424]

Csicsvari J, Jamieson B, Wise KD, Buzsaki G. Mechanisms of gamma oscillations in the hippocampus of the behaving rat. Neuron 2003;37:311–322. [PubMed: 12546825]

Deacon RM, Bannerman DM, Rawlins JN. Anxiolytic effects of cytotoxic hippocampal lesions in rats. Behav Neurosci 2002;116:494–497. [PubMed: 12049331]

DeCoteau WE, Thorn C, Gibson DJ, Courtemanche R, Mitra P, Kubota Y, Graybiel AM. Learning-related coordination of striatal and hippocampal theta rhythms during acquisition of a procedural maze task. Proc Natl Acad Sci U S A 2007;104:5644–5649. [PubMed: 17372196]

Fee JR, Sparta DR, Knapp DJ, Breese GR, Picker MJ, Thiele TE. Predictors of high ethanol consumption in RIIbeta knock-out mice: assessment of anxiety and ethanol-induced sedation. Alcohol Clin Exp Res 2004;28:1459–1468. [PubMed: 15597077]

File SE, Gonzalez LE, Andrews N. Comparative study of pre- and postsynaptic 5-HT1A receptor modulation of anxiety in two ethological animal tests. J Neurosci 1996;16:4810–4815. [PubMed: 8764667]

Gloveli T, Dugladze T, Rotstein HG, Traub RD, Monyer H, Heinemann U, Whittington MA, Kopell NJ. Orthogonal arrangement of rhythm-generating microcircuits in the hippocampus. Proc Natl Acad Sci U S A 2005;102:13295–13300. [PubMed: 16141320]

Gonzalez LE, Rujano M, Tucci S, Paredes D, Silva E, Alba G, Hernandez L. Medial prefrontal transection enhances social interaction. I: behavioral studies. Brain Res 2000;887:7–15. [PubMed: 11134584]

Gordon JA, Lacefield CO, Kentros CG, Hen R. State-dependent alterations in hippocampal oscillations in serotonin 1A receptor-deficient mice. J Neurosci 2005;25:6509–6519. [PubMed: 16014712]

Gross C, Zhuang X, Stark K, Ramboz S, Oosting R, Kirby L, Santarelli L, Beck S, Hen R. Serotonin1A receptor acts during development to establish normal anxiety-like behaviour in the adult. Nature 2002;416:396–400. [PubMed: 11919622]

Heisler LK, Chu HM, Brennan TJ, Danao JA, Bajwa P, Parsons LH, Tecott LH. Elevated anxiety and antidepressant-like responses in serotonin 5-HT1A receptor mutant mice. Proc Natl Acad Sci U S A 1998;95:15049–15054. [PubMed: 9844013]

Hoover WB, Vertes RP. Anatomical analysis of afferent projections to the medial prefrontal cortex in the rat. Brain Struct Funct 2007;212:149–179. [PubMed: 17717690]

Hyman JM, Zilli EA, Paley AM, Hasselmo ME. Medial prefrontal cortex cells show dynamic modulation with the hippocampal theta rhythm dependent on behavior. Hippocampus 2005;15:739–749. [PubMed: 16015622]

Jones MW, Wilson MA. Theta rhythms coordinate hippocampal-prefrontal interactions in a spatial memory task. PLoS Biol 2005;3:e402. [PubMed: 16279838]

Kjelstrup KB, Solstad T, Brun VH, Hafting T, Leutgeb S, Witter MP, Moser EI, Moser MB. Finite scale of spatial representation in the hippocampus. Science 2008;321:140–143. [PubMed: 18599792]

Kjelstrup KG, Tuvnes FA, Steffenach HA, Murison R, Moser EI, Moser MB. Reduced fear expression after lesions of the ventral hippocampus. Proc Natl Acad Sci U S A 2002;99:10825–10830. [PubMed: 12149439]

Klemenhagen KC, Gordon JA, David DJ, Hen R, Gross CT. Increased fear response to contextual cues in mice lacking the 5-HT1A receptor. Neuropsychopharmacology 2006;31:101–111. [PubMed: 15920501]

Lacroix L, Broersen LM, Weiner I, Feldon J. The effects of excitotoxic lesion of the medial prefrontal cortex on latent inhibition, prepulse inhibition, food hoarding, elevated plus maze, active avoidance and locomotor activity in the rat. Neuroscience 1998;84:431–442. [PubMed: 9539214]

Lacroix L, Spinelli S, Heidbreder CA, Feldon J. Differential role of the medial and lateral prefrontal cortices in fear and anxiety. Behav Neurosci 2000;114:1119–1130. [PubMed: 11142644]

Lister RG. The use of a plus-maze to measure anxiety in the mouse. Psychopharmacology (Berl) 1987;92:180–185. [PubMed: 3110839]

McNaughton N, Gray JA. Anxiolytic action on the behavioural inhibition system implies multiple types of arousal contribute to anxiety. J Affect Disord 2000;61:161–176. [PubMed: 11163419]

Parent MA, Wang L, Su J, Netoff T, Yuan LL. Identification of the Hippocampal Input to Medial Prefrontal Cortex In Vitro. Cereb Cortex. 2009

Parks CL, Robinson PS, Sibille E, Shenk T, Toth M. Increased anxiety of mice lacking the serotonin1A receptor. Proc Natl Acad Sci U S A 1998;95:10734–10739. [PubMed: 9724773]

Puumala T, Sirvio J. Changes in activities of dopamine and serotonin systems in the frontal cortex underlie poor choice accuracy and impulsivity of rats in an attention task. Neuroscience 1998;83:489–499. [PubMed: 9460757]

Ramboz S, Oosting R, Amara DA, Kung HF, Blier P, Mendelsohn M, Mann JJ, Brunner D, Hen R. Serotonin receptor 1A knockout: an animal model of anxiety-related disorder. Proc Natl Acad Sci U S A 1998;95:14476–14481. [PubMed: 9826725]

Resstel LB, Souza RF, Guimaraes FS. Anxiolytic-like effects induced by medial prefrontal cortex inhibition in rats submitted to the Vogel conflict test. Physiol Behav 2008;93:200–205. [PubMed: 17884112]

Seidenbecher T, Laxmi TR, Stork O, Pape HC. Amygdalar and hippocampal theta rhythm synchronization during fear memory retrieval. Science 2003;301:846–850. [PubMed: 12907806]

Shah AA, Sjovold T, Treit D. Inactivation of the medial prefrontal cortex with the GABAA receptor agonist muscimol increases open-arm activity in the elevated plus-maze and attenuates shock-probe burying in rats. Brain Res 2004;1028:112–115. [PubMed: 15518648]

Shah AA, Treit D. Excitotoxic lesions of the medial prefrontal cortex attenuate fear responses in the elevated-plus maze, social interaction and shock probe burying tests. Brain Res 2003;969:183–194. [PubMed: 12676379]

Shah AA, Treit D. Infusions of midazolam into the medial prefrontal cortex produce anxiolytic effects in the elevated plus-maze and shock-probe burying tests. Brain Res 2004;996:31–40. [PubMed: 14670628]

Siapas AG, Lubenov EV, Wilson MA. Prefrontal phase locking to hippocampal theta oscillations. Neuron 2005;46:141–151. [PubMed: 15820700]

Sirota A, Buzsaki G. Interaction between neocortical and hippocampal networks via slow oscillations. Thalamus Relat Syst 2005;3:245–259. [PubMed: 18185848]

Sirota A, Montgomery S, Fujisawa S, Isomura Y, Zugaro M, Buzsaki G. Entrainment of neocortical neurons and gamma oscillations by the hippocampal theta rhythm. Neuron 2008;60:683–697. [PubMed: 19038224]

Sustkova-Fiserova M, Vavrova J, Krsiak M. Brain levels of GABA, glutamate and aspartate in sociable, aggressive and timid mice: an in vivo microdialysis study. Neuro Endocrinol Lett 2009;30:79–84. [PubMed: 19300401]

Szabadics J, Lorincz A, Tamas G. Beta and gamma frequency synchronization by dendritic gabaergic synapses and gap junctions in a network of cortical interneurons. J Neurosci 2001;21:5824–5831. [PubMed: 11466454]

Thierry AM, Gioanni Y, Degenetais E, Glowinski J. Hippocampo-prefrontal cortex pathway: anatomical and electrophysiological characteristics. Hippocampus 2000;10:411–419. [PubMed: 10985280]

Tierney PL, Degenetais E, Thierry AM, Glowinski J, Gioanni Y. Influence of the hippocampus on interneurons of the rat prefrontal cortex. Eur J Neurosci 2004;20:514–524. [PubMed: 15233760]

Vertes RP. Differential projections of the infralimbic and prelimbic cortex in the rat. Synapse 2004;51:32–58. [PubMed: 14579424]

Verwer RW, Meijer RJ, Van Uum HF, Witter MP. Collateral projections from the rat hippocampal formation to the lateral and medial prefrontal cortex. Hippocampus 1997;7:397–402. [PubMed: 9287079]

Vidal-Gonzalez I, Vidal-Gonzalez B, Rauch SL, Quirk GJ. Microstimulation reveals opposing influences of prelimbic and infralimbic cortex on the expression of conditioned fear. Learn Mem 2006;13:728–733. [PubMed: 17142302]

Yee BK. Cytotoxic lesion of the medial prefrontal cortex abolishes the partial reinforcement extinction effect, attenuates prepulse inhibition of the acoustic startle reflex and induces transient hyperlocomotion, while sparing spontaneous object recognition memory in the rat. Neuroscience 2000;95:675–689. [PubMed: 10670435]

Zhu XO, McNaughton N. Effects of long-term administration of antidepressants on septal driving of hippocampal RSA. Int J Neurosci 1994;79:91–98. [PubMed: 7744554]

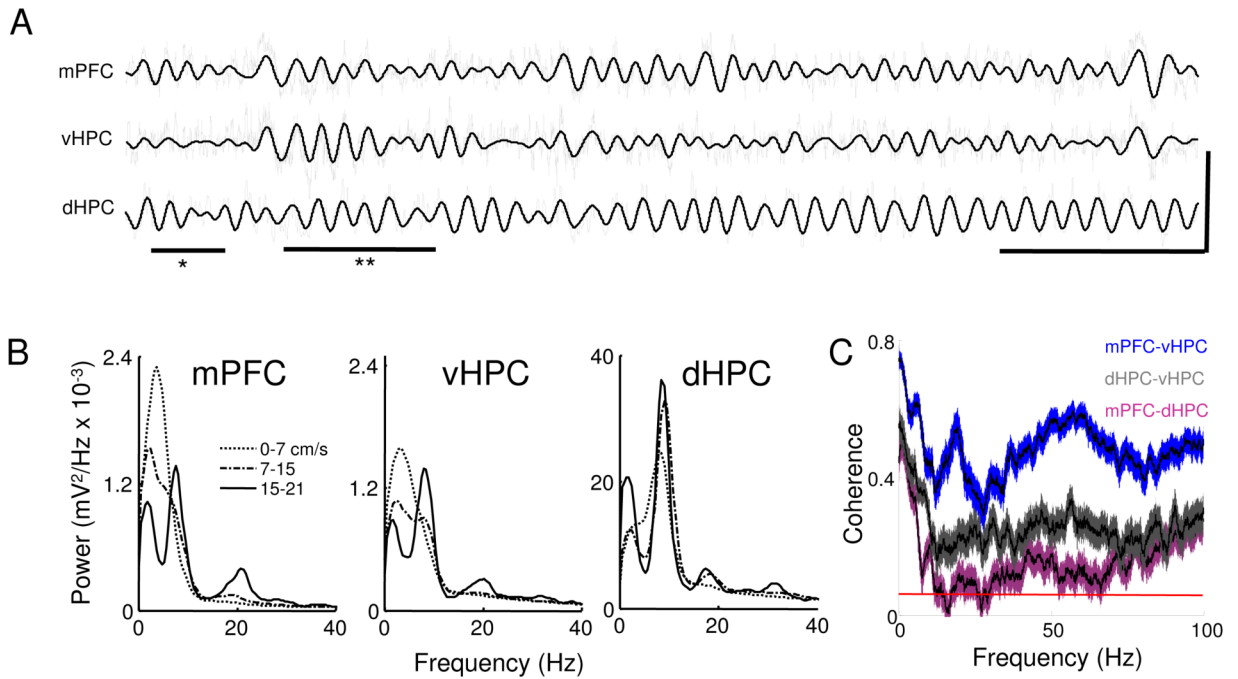**Figure 1. Characterization of LFPs from the mPFC, vHPC and dHPC in the familiar arena**
(A) Traces of simultaneously recorded local field potentials from the mPFC, vHPC and dHPC
in a mouse exploring the familiar arena. Raw traces are plotted in grey and theta filtered traces
are overlaid in black. Underlines indicate a period robust theta activity in mPFC with minimal
theta in the vHPC (*) and a period of robust theta-range activity in both mPFC and vHPC (**).
Calibration: horizontal bar:1 s, vertical bar: 0.5 mV for mPFC and vHPC and 2.5 mV for dHPC
trace. (B) Power spectra for different speed ranges for mPFC, vHPC and dHPC. Note that the
peak centered at the theta range increases with higher speeds in all three areas. Also note the
different scale on dHPC figure; theta power is much higher in dHPC than in vHPC and mPFC.
Spectra are averages of 13 animals. (C) Coherence averaged across animals for mPFC-vHPC
(blue), mPFC-dHPC (purple) and vHPC-dHPC (grey) recorded in the 7-15 cm/s speed range.
Note that mPFC-vHPC coherence is higher than mPFC-dHPC for all frequencies. Shaded areas
indicate 95% confidence intervals and the red line at the bottom shows the coherence expected
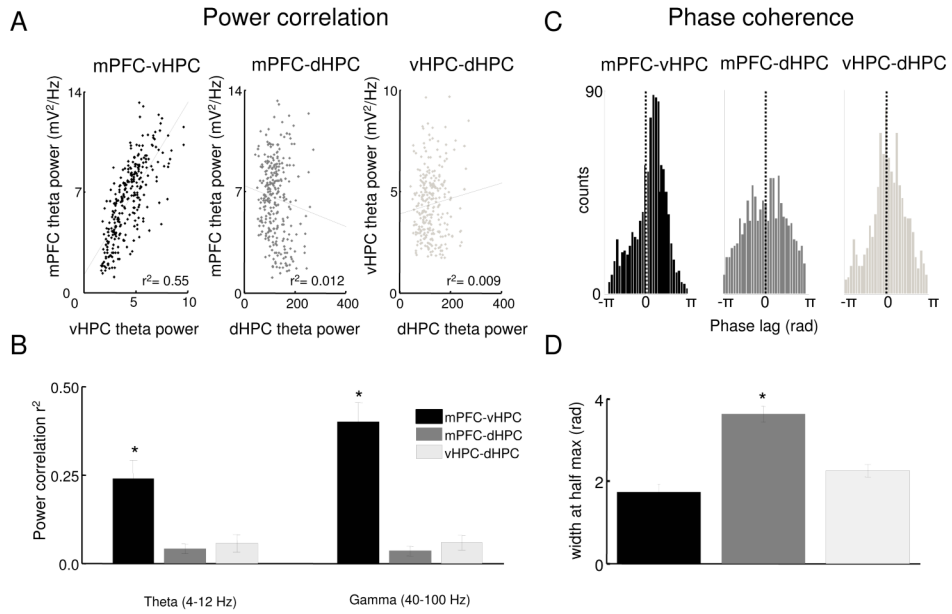by chance (p<0.05). See also Figures S1, S7 and S8.

Figure 2. Power correlations and phase coherence across areas
(A) Representative examples of theta power correlation scatter plots for vHPC-mPFC, dHPC-mPFC and vHPC-dHPC from a 10 minute recording session in the familiar arena. Each data point represents the sum of theta power during a 2.6 s window. (B) Averages of the linear correlation coefficients of theta (left corner) and gamma (right corner) power across 13 animals for vHPC-mPFC, dHPC-mPFC and vHPC-dHPC. Error bars are ± s.e.m. *p<0.01 for paired t-tests on the Fisher's Z-transformed r values compared to mPFC-vHPC. (C) Representative histogram of theta phase differences. Instantaneous theta phase of two signals were subtracted from each other and the difference in theta phase was plotted as a histogram, for mPFC-vHPC (black), mPFC-dHPC (dark grey) and dHPC-vHPC (light grey). Narrower peaks in the histogram indicate a more consistent phase relationship. (D) Width of theta phase difference histogram at half of the peak height averaged across 13 animals for vHPC-mPFC (right panel), dHPC-mPFC (center panel) and vHPC-dHPC (left panel). Error bars are ± s.e.m. *p<0.01 for t-test comparing mPFC-vHPC to mPFC-dHPC.
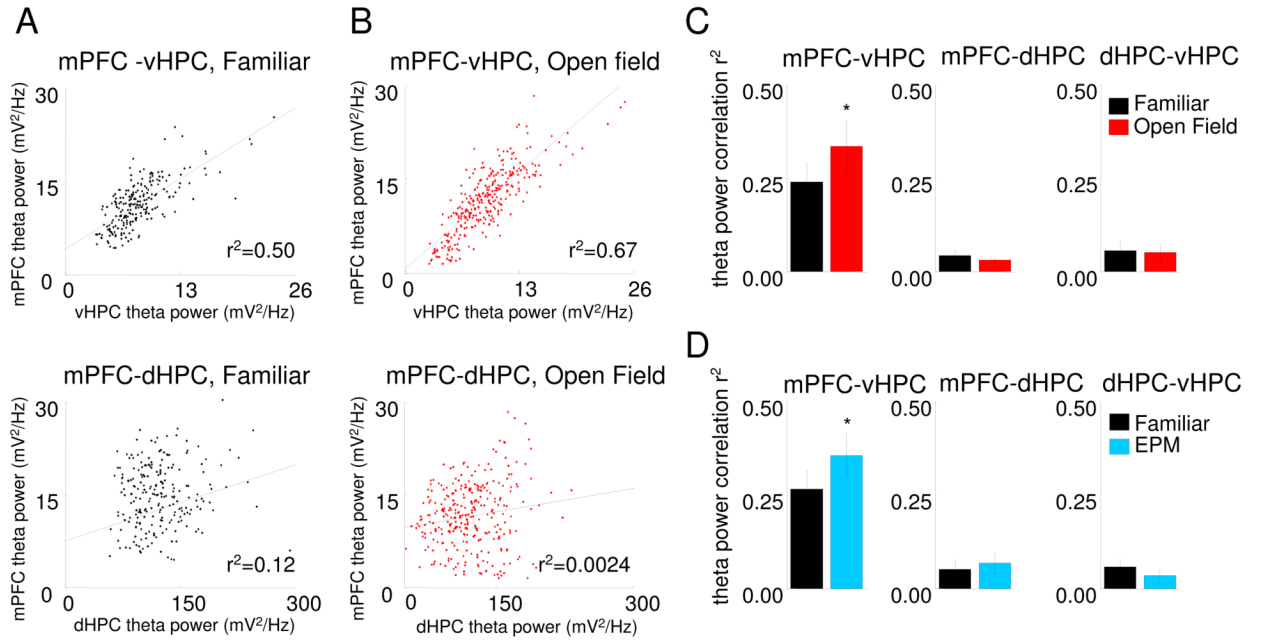
Figure 3. Theta power correlation between mPFC and vHPC increases in the EPM and open field
(A) Representative example of theta power correlation plot in the familiar arena between mPFC and vHPC (upper panel) and dHPC (lower panel). (B) Theta power correlation plot in the open field from the same animal as in Fig. 4a between mPFC and vHPC (upper panel) and the dHPC (lower panel). Note the increase in mPFC-vHPC linear correlation r^2 compared to Figure 4 A. Changes in averaged r^2 of theta power correlations between in the familiar arena and open field (C) and EPM D) for mPFC-vHPC (left panel), mPFC-dHPC (middle panel) and dHPC-vHPC (right panel). Bars are averages of data from 13 animals, error bars are ± s.e.m. *p<0.05 for a paired t-test for the Fisher's Z transformed r values. See also Figures S2, S3 and S4.
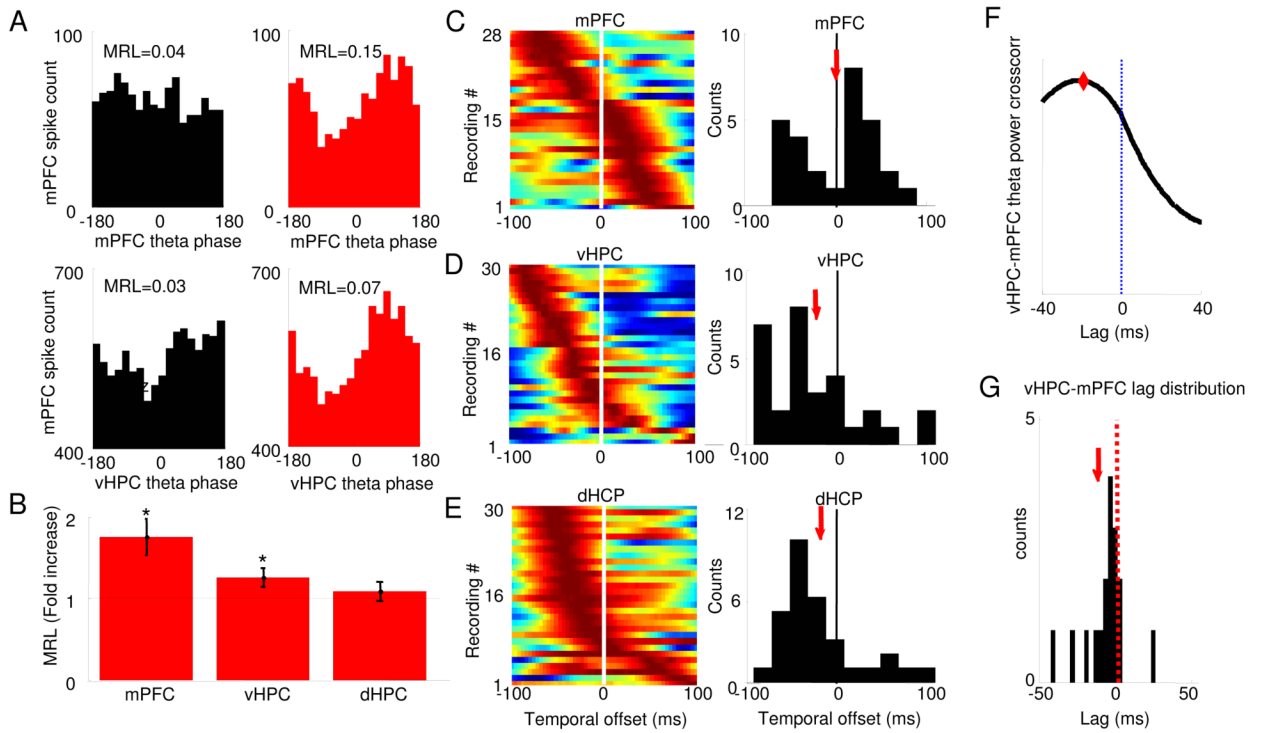
Figure 4. Multiunit phase-locking to mPFC and vHPC theta increases in the open field
(A) Representative examples of the distribution of preferred phases of multiunit activity recorded in the mPFC relative to local (upper panels) and vHPC (lower panels) theta oscillations in the familiar arena (black histograms) and the open field (red histograms). (B) Mean +/− S.E.M. of MRL values in the open field relative to the familiar environment for multiunit recordings to mPFC (left bar), vHPC (middle) and dHPC (right) theta oscillations. Note that the MRL in the open field is larger than in the familiar arena, indicating more robust phase-locking to both mPFC and vHPC theta oscillations. (C-E). mPFC units phase lock best to local theta of the present (C) and hippocampal theta o f the past (D,E). Color-coded plots show changes in MRL values for multiunit recordings after spikes are shifted in time relative to theta oscillations of mPFC (C), vHPC (D) and dHPC (E). Higher MRL values correspond to warmer colors. Each row corresponds to one multiunit recording. Rows are arranged according to the temporal offsets that produce maximal phase locking. Upper rows correspond to multiunit recordings that phase lock most robustly with large negative shifts, i.e., maximal phase locking to theta of the past. Histograms showing the population distribution of the temporal offsets with highest phase locking are shown on the right. The population mean is indicated by red arrows. Note that on average spikes in the mPFC are most strongly phase locked to hippocampal theta of theta of the past. Only recordings that were significantly phase locked (by Rayleigh's test for circular uniformity, Bonferroni corrected $p < 0.05/40$) in at least one temporal shift were used. n=28-30 multiunit recordings. *$p<0.05$ for a paired Wilcoxon's signed rank test on MRL values. (F) Example of crosscorrelation of mPFC and vHPC theta power. Note that the crosscorrelation peaks at a negative lag, indicating that theta power changes occur first in the vHPC and then in the mPFC. Instantaneous power was calculated through the Hilbert transform. (G) Histogram showing the distribution of lags with maximal crosscorrelation across animals. The median lag is significantly different from zero (−8 ms, $p<0.05$, signrank test). Only segments of data where vHPC theta power was greater than the mean vHPC theta power for a given session were used. The population mean is indicated by a red arrow.
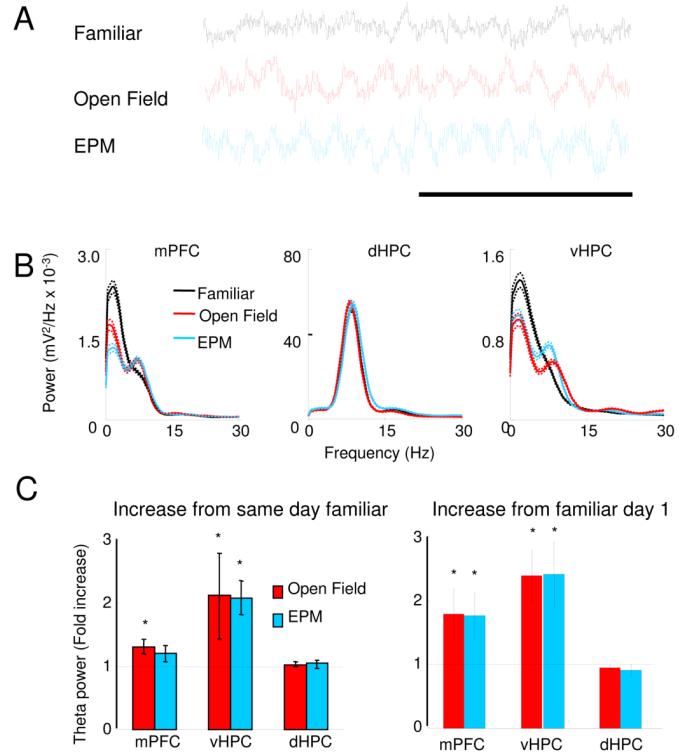
Figure 5. Theta power in the mPFC and dHPC increases during exposure to the EPM and open field

(A) Representative traces of mPFC LFPs recorded from the same animal in the familiar arena, open field and EPM. Calibration: 1s. (B) Examples of representative power spectra in the familiar arena (black traces), open field (red) and EPM (blue) from LFPs of the mPFC (left panel), vHPC (center) and dHPC (right). Mean power was calculated using the Welch method with s.e.m. (dashed lines) calculated across windows. (C) Left panel: Fold increases in theta power relative to the familiar arena exposures obtained in the same day as the open field (red bars) and in the EPM (blue bars) recordings. Right panel: Same as left panel, but relative to the first day of exposure to the familiar environment. All data are taken from epochs in which animals were running consistently in the 7-15 cm/s speed range. See also Figures S5 and S9.
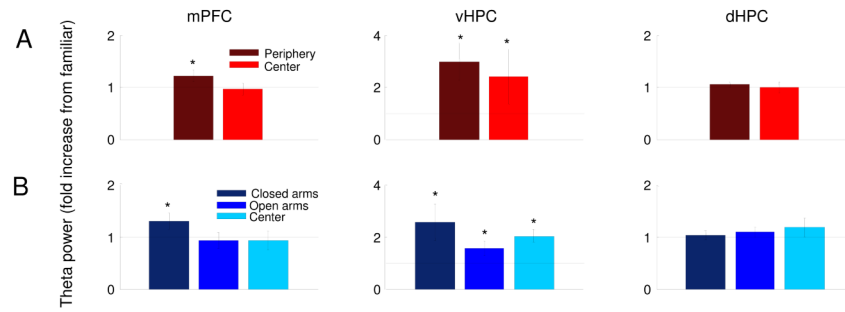
Figure 6. mPFC theta power is increased specifically in the safe zones of the anxiogenic arenas
(A) Theta power increases in the mPFC, vHPC and dHPC during navigation of the periphery (dark red) and center (bright red) of the open field. (B) Theta power increase in each area during navigation of the closed arms (dark blue), open arms (medium blue), and center (light blue) of the elevated plus maze. n=18 and 12 for the open field and EPM, respectively. All data are from epochs in which animals were running consistently in the 7-15 cm/s speed range. Fold increases are relative to theta power in the familiar arena exposure on the same day. Error bars are ± s.e.m. *$p < 0.05$, for a paired Wilcoxon's signed rank test.
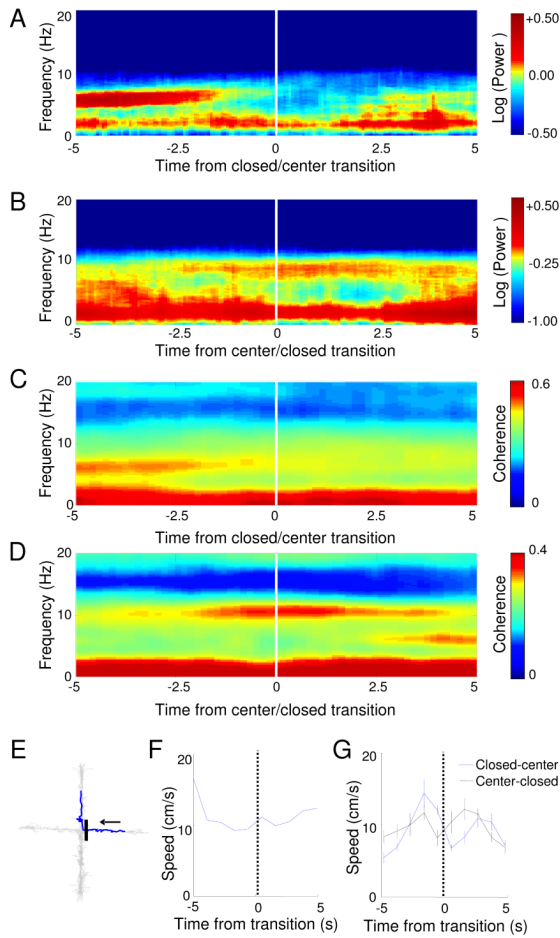
Figure 7. mPFC theta power and mPFC-vHPC coherence increase prior to leaving the closed arms
(A) Average mPFC spectrogram of all closed arm to center transitions in the EPM, centered at the transition point (time=0 sec). (B) Same as (A), but for center to closed arm transitions. Note sharp changes in mPFC theta power occur 2-3 s before the animal enters a new compartment of the maze. (C) Average mPFC-vHPC coherence centered at the closed to center transition. (D) Same as (C), but for center to closed transitions. (E) Example track of a closed to center transition. 10 seconds of movement (blue trace) centered at the transition is shown. Grey trace tracks the position of the mouse in the entire session. The black bar indicates the position of the transition, and the arrow shows the direction of movement. (F) Speed across time for the example transition shown in (E). (G) Average speed for both closed to center and center to closed transitions is shown.
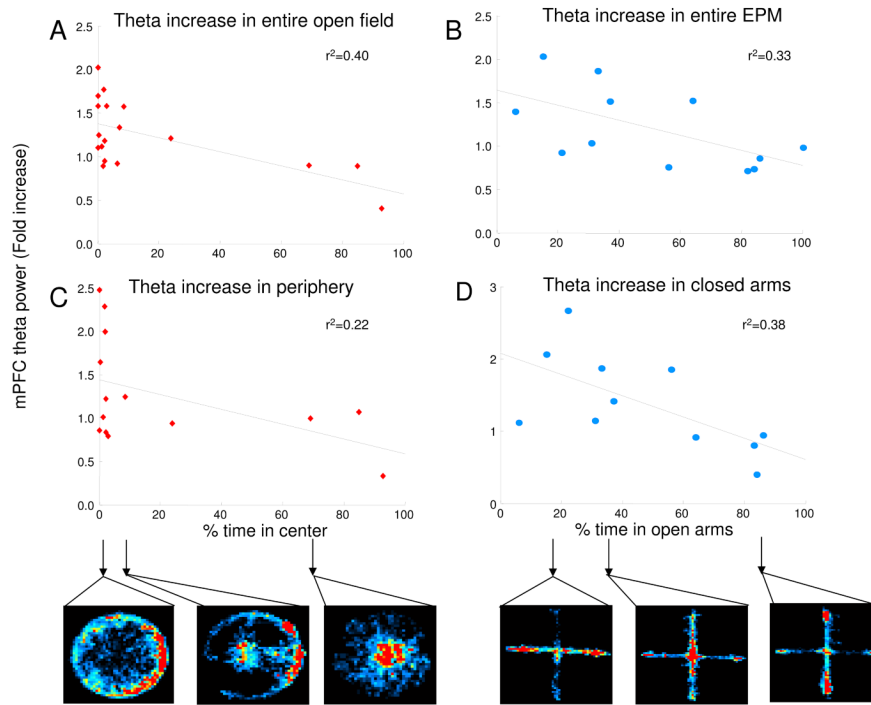
Figure 8. mPFC theta power increases in the EPM and the open field correlate with behavioral measures of anxiety

(A,B) Scatter plots of mPFC fold theta increase relative to the familiar arena against % time spent in the center of the open field, (A) and % time in the open arms for the EPM, (B). (C,D) Plots of fold increases in theta power in the periphery of the open field and in the closed arms of the EPM relative to the familiar environment recording of the same day, as a function of anxiety-associated behaviors in the open field (C) and the EPM (D). Lower panels show movement tracks as heat maps for selected points, indicated by arrows. In the maps of the EPM, open arms are vertically oriented. Fold theta power changes were calculated from epochs in which animals were running consistently in the 7-15 cm/s speed range.
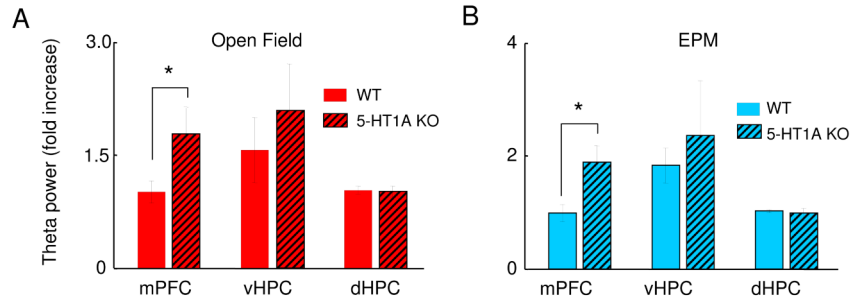
Figure 9. 5-HT1A knockouts (5-HT1A KO) have a higher increase in mPFC theta power in the EPM and the open field relative to wildtype (WT) mice
Bar graphs of average fold theta increase in the mPFC (left), vHPC (center) and dHPC (right), for the open field (red bars, upper panel) and EPM (blue bars, lower panel). Bars represent averages of 7 WT (clear bars) and 7 5-HT1A KO (thatched bars) mice. Error bars are ± s.e.m. *p<0.05 for a paired Wilcoxon's signed rank test comparing the fold theta increases of WT and 5-HT1A KO animals. Fold theta power changes were calculated from epochs in which animals were running consistently in the 7-15 cm/s speed range.